Response of Distribution Feeder Microgrids to System-Level Reserve Requests

Yasser Yasaei
Dept. of Electrical and Computer Engineering
University of New Mexico
Albuquerque, New Mexico
Email:yasaei@unm.edu

Majeed M. Hayat
Dept. of Electrical and Computer Engineering
University of New Mexico
Albuquerque, New Mexico
Email:hayat@unm.edu

Andrea A. Mammoli
Dept. of Mechanical Engineering
University of New Mexico
Albuquerque, New Mexico
Email:mammoli@unm.edu

***Abstract*—The ability of distribution feeder microgrids to operate as a controllable entity and participate in system-level services is assessed in this paper. The concept of distribution feeder microgrid is introduced. A control mechanism that fits this architecture and fulfills performance criteria as well as stability requirements is discussed in detail. Distribution feeder microgrids when equipped with the proposed control mechanism is shown to have the potential for increasing the heterogeneity of generation-mix and unveiling the hidden capacity of under-utilized resources that can be used in essential power system services. Simulation results verify the envisioned advantages of the application.**

I. Introduction

The observed fragility of the current power system infrastructure has raised many questions about its resiliency in a future in which severe weather and events and malicious attacks are likely to be more frequent [1]. There is also a growing trend for deploying distributed resources due to environmental concerns as well as financial incentives. These resources include photovoltaic (PV) power generation, building energy systems and storage devices.

The intermittent nature of renewable resources, however, places a barrier on their deployment beyond certain levels [2]. New solutions, both infrastructure-centered and control mechanism-centered, are needed to go beyond current limits. We propose a control framework and a system architecture to fully leverage the potential of distributed resources.

A microgrid-based architecture for a power grid is a viable platform for our purposes. The utility distribution microgrid is of interest in this study. In this structure, feeders that adopt this architecture will provide levels of controllability which are able to facilitate useful services to future power systems with high levels of renewable penetration. An example is the Borrego Springs microgrid, owned by SDG&E utility company, which enables integration of a large amount of intermittent PV power generation. This microgrid can be either connected to the grid or work in an island mode if needed [3].

The control mechanism consists of two separate optimization processes. A day-ahead scheduling problem is in charge of determining optimal operating points for various resources throughout a day. This optimized schedule is then combined with a dynamic programming process, known as model predictive control (MPC), to account for real-time deviations from day-ahead forecasts [4], [5]. These deviations are fluctuations in both the generated power from renewable resources as well as the demand.

In the current system, large-scale generation fills the gap between loads and intermittent renewable generation. It is able to do that because of large amounts of rotating mass. As large rotating mass is displaced by intermittent generation at the transmission and distribution levels, the ability of the grid to remain stable may be compromised. The framework presented here turns the problem upside down. Rather than relying on large inertia in the generation system, stability is maintained by distribution feeders designed as controllable entities capable of absorbing intermittency. The ability of distribution feeder microgrids to perform this function results from a combination of storage and control. Storage resources are heterogeneous. Examples include battery systems, thermal storage devices and even the thermal mass of buildings.

Despite their differences, all resources can be categorized by their energy capacity, their power capacity and their ramping capacity. Resources with similar characteristics can be associated with a specific task. For instance, fast-ramping resources can be used to absorb high-frequency intermittency, while slow but high-energy resources can be used to meet the mismatch between peak load and peak solar generation. As an example of the ability of this new architecture to provide grid services, we use distribution feeder microgrids to serve regulating services. We show how the scheduling/MPC framework can readily adapt to this task.

The main contribution of this paper is two-faceted. First, we pair the performance specifications of a resource with the appropriate problem (e.g., slow, high-energy thermal storage to peak-shifting). The second facet is that we propose a financially meaningful cost function for the dynamic programming problem (MPC). This is in contrast to the typical quadratic cost functions that researchers use when employing MPC framework [5].

II. Modeling Energy Storage Devices

Implementation of the scheduling and MPC algorithms discussed in section I requires a unified framework to model the heterogeneous distributed resources that are present within a distribution feeder. In this framework, all resources are characterized by energy capacity, power capacity and ramping

rate. The state of each device at time step k can be described by a 2×1 vector $\boldsymbol{x}_k = (E_k, P_k)^T$, where E_k is the energy stored at time step k, and P_k is the instantaneous output power. Negative power usually implies charging of a storage device.

Additionally, we assume that devices are controlled by a ramp rate input signal, which is the time derivative of the power signal. Given that the power P_k is the time derivative of energy, each storage device can be described by a second-order dynamical model. The three variables energy, power and ramp rate are associated with constraints that determine the specifications of a device. Each distributed resource is characterized by an energy storage capacity. For the case of a battery, this may be a finite limit, while a fuel cell powered by natural gas has unlimited storage capacity. Power input or output of devices is similarly constrained, as is ramp rate capacity.

In summary, the dynamical model of each storage device is described by a second-order difference equation

$$\begin{pmatrix} E_{k+1} \\ P_{k+1} \end{pmatrix} = \begin{pmatrix} 1 & -t_s \\ 0 & 1 \end{pmatrix} \begin{pmatrix} E_k \\ P_k \end{pmatrix} + \begin{pmatrix} -t_s^2/2 \\ t_s \end{pmatrix} u_k, \quad (1)$$

where t_s is the sampling time, and

$$\begin{array}{rcccl} 0 & \leq & E_k & \leq & E_{\text{max}}, \\ P_{\text{min}} & \leq & P_k & \leq & P_{\text{max}}, \\ u_{\text{min}} & \leq & u_k & \leq & u_{\text{max}}. \end{array} \quad (2)$$

The signal u_k is the ramp rate associated with the device. As discussed in the previous section, storage devices of interest in this study include but are not confined to conventional ones. Specifically, we see an opportunity in deploying unconventional and generally under-utilized resources rather than simply electrical storage for our control purposes. For example, thermal mass associated with commercial-size building heating, ventilation and air conditioning (HVAC) systems or aggregated storage associated with residential thermostatically controlled loads (TCLs) are two instances of the available facilities that can find dual use as distributed resources [6].

III. Control Mechanism

Large scale adoption of feeder microgrids would shift the current centralized generation paradigm to a more decentralized one, which relies more heavily on renewable resources. Consequently, the control infrastructure and mechanisms should also be changed to suit this paradigm shift. The increased penetration of distributed resources requires an increased level of decentralized control. A two-level optimization approach that is implemented on a distribution feeder microgrid is proposed here: a day-ahead scheduling combined with an MPC framework. The former is a single shot optimization that takes place every 24 hours, while the latter is a dynamic programming problem that balances resources in real-time.

The day-ahead scheduling optimization occurs daily to determine the set points of devices with 60 minutes time resolution, that minimize operating costs. The optimization is based on load and resource forecasts as well as energy tariff structures. At a lower level, the MPC framework is applied to compensate for real-time deviations from forecast values.

The optimal day-ahead scheduling process is beyond the scope of this paper. We assume that an optimized schedule is made available by either an on-site or a cloud-based service, e.g. Toshiba's micro-energy management system (μEMS) for the former [7] and Lawrence Berkeley national lab's Distributed Energy Resource Customer Adoption Model (DER-CAM) for the latter [8].

Because no forecast is perfectly accurate, it is necessary to make real-time adjustments that simultaneously minimize the cost of deviations from the original schedule, maintain stability and balance power flow. A model predictive algorithm is used for this purpose. In this control technique, an optimization problem is solved at each time step to specify a set of control actions over a future period of time. The first calculated control action, then, is applied at each time step to the system. The process is repeated at each successive time step taking into account the current state as well as the updated estimates of future quantities. The control policy is evidently a feedback system as it uses the current system state at each time step [4]. While the cost function in the day-ahead scheduling reflects absolute costs, in the MPC process costs are those associated with deviations from the optimized schedule. These costs can be written as:

$$J_{\text{MPC}} = \sum_{k=0}^{N} l(\boldsymbol{x}_k - \boldsymbol{x}_{sch,k}, \boldsymbol{u}_k - \boldsymbol{u}_{sch,k}), \quad (3)$$

where $\boldsymbol{x}_k$ is the state, and $\boldsymbol{u}_k$ is the control input at the time step k. The state vector $\boldsymbol{x}_k$ is the $2m \times 1$ column-vector of aggregated state vectors $\boldsymbol{x}_{i,k}$: $i = 1, \ldots, m$ associated with each of the m available resources as $\boldsymbol{x}_k = (\boldsymbol{x}_{1,k}^T \ldots \boldsymbol{x}_{m,k}^T)^T$. In the same fashion, the $m \times 1$ control input $\boldsymbol{u}_k$ is composed of the single control input of each of the devices as $\boldsymbol{u}_k = (u_{1,k} \ldots u_{m,k})^T$. Moreover, the signals $\boldsymbol{x}_{sch,i}$ and $\boldsymbol{u}_{sch,i}$ are the corresponding scheduled values.

Rewriting the difference equation (1) as $\boldsymbol{x}_{i,k+1} = A_i \boldsymbol{x}_{i,k} + B_i \boldsymbol{u}_{i,k}$ and forming the corresponding matrices A_i and B_i, the aggregated dynamics $\boldsymbol{x}_{k+1} = A\boldsymbol{x}_k + B\boldsymbol{u}_k$ can be described by

$$\begin{aligned} A &= \begin{pmatrix} A_1 & \mathbf{0} & \ldots & \mathbf{0} \\ \mathbf{0} & A_2 & \ldots & \mathbf{0} \\ \vdots & \vdots & \ddots & \vdots \\ \mathbf{0} & \mathbf{0} & \ldots & A_m \end{pmatrix}, \\ B &= \begin{pmatrix} B_1 & \mathbf{0} & \ldots & \mathbf{0} \\ \mathbf{0} & B_2 & \ldots & \mathbf{0} \\ \vdots & \vdots & \ddots & \vdots \\ \mathbf{0} & \mathbf{0} & \ldots & B_m \end{pmatrix}. \end{aligned} \quad (4)$$

The aggregated dynamics, in fact, act as a constraint on the dynamic programming problem, the cost function of which is stated in the eq. (3). In addition to the dynamics of the system and the associated physical constraints of the resources (shown in eq. (2)), another constraint should be added to the optimization problem. This constraint results from the

requirement that the demand is perfectly met by the available resources on the microgrid or in combination with a share from the grid. This translates into the following equality constraint for the dynamic programming problem of interest as:

$$\underbrace{(0\ 1\ \ldots\ 0\ 1)}_{2m\times 1}\cdot \boldsymbol{x}_k = P_{\text{ref},k}, \tag{5}$$

where $P_{\text{ref},k}$ is the reference power demand at time step k.

Usually, the objective function of an MPC problem is a summation of various quadratic costs, e.g. in the MPC approach used by Anderson [5]. These kinds of costs result in a convex optimization objective, provided that the associated constraints satisfy the convexity conditions as well. The wide availability of quadratic solvers makes this approach attractive. A general form of such a cost function can be mathematically formulated as:

$$\begin{aligned} J_{\text{MPC}} = \sum_{k=0}^{N} \quad & (\boldsymbol{x}_k - \boldsymbol{x}_{\text{sch},k})^T Q_k (\boldsymbol{x}_k - \boldsymbol{x}_{\text{sch},k}) + \\ & (\boldsymbol{u}_k - \boldsymbol{u}_{\text{sch},k})^T R_k (\boldsymbol{u}_k - \boldsymbol{u}_{\text{sch},k}). \end{aligned} \tag{6}$$

Although this class of cost functions has been widely adopted because of its attractive features, it often does not reflect real costs in the field. For example, the cost of fuel for internal combustion engines or fuel cells is better approximated by linear functions, while the degradation cost of a battery which reflects the fact that the device degrades independently of the direction of power flow, is well-approximated by absolute value functions. Thus, in our study , the cost function is a summation of linear and absolute value costs, and can be represented as

$$J_{\text{MPC}} = \sum_{k=0}^{N} Q_k^T (E_k - E_{k+1}) + Q_k^{'T} |E_k - E_{k+1}|. \tag{7}$$

The objective function of eq.(7) combined with eqs.(2), (4) and (5), that meet convexity criteria, makes the proposed dynamic programming a convex optimization problem.

The MATLAB optimization toolbox contains a general yet powerful function, named *fmincon*. This solver, however, is not fast enough based on the fact that it has been designed for general optimization problems. Instead, we utilize *CVX*, an open-source toolbox for convex optimization problems available in public domain [9], [10]. This toolbox is developed for disciplined convex programming, and thus, a good candidate for our developed convex problem. Although, we developed our application around this package, we used *fmincon* for verification.

IV. Resource Characteristics and Cascading Model Predictive Control

Deviations from the schedule are mainly the consequence of the fluctuations associated with either the load or renewable power generation. The MPC process optimally dispatches resources to compensate the mismatch between forecasts and actual system state values. Because the number of resources could be large, solution of this problem could become computationally expensive. To reduce the size of the problem, we match the characteristics of each resource to an appropriate part of the mismatch frequency spectrum.

Some resources are able to respond effectively to rapid variations, while some others are too slow. On the other hand, fast devices do not have significant storage capacity in general which constraints their usefulness in applications where sustained power delivery or absorption is required. Slow devices, such as energy batteries or thermal storage systems are well-matched to the low-frequency part of the real-time versus schedule mismatch spectrum. Thus, decomposition of the deviations into various frequency bands seems reasonable.

The reference signal that must be tracked by resources dispatch by the MPC controller results from the net effect of deviation of renewable generation and the load from their schedule counterparts. For reasons of computational efficiency, we use a real-time digital series filter to decompose the mismatch signal into three frequency bands. The linear filter of interest has the general form of

$$y_n = \sum_{k=0}^{L} c_k z_{n-k} + \sum_{j=1}^{L} d_j y_{n-j}, \tag{8}$$

takes a sequence of input sequence $\{z_n\}$ and produces the output sequence $\{y_n\}$ [11]. In this study, $L = 2$ and $M = 1$. For a band-pass filter with the lower and upper bands a and b, respectively, the appropriate coefficients c_ks and d_js are determined as

$$\begin{aligned} c_0 &= -\tfrac{b}{(1+a)(1+b)}, \\ c_1 &= 0, \\ c_2 &= \tfrac{b}{(1+a)(1+b)}, \\ d_1 &= \tfrac{(1+a)(1-b)+(a-1)(1+b)}{(1+a)(1+b)}, \\ d_2 &= -\tfrac{(1-a)(1-b)}{(1+a)(1+b)}. \end{aligned} \tag{9}$$

that results in the transfer function

$$\mathcal{H}(f) = (\frac{\omega}{\omega - ja})(\frac{jb}{\omega - jb}), \tag{10}$$

with the poles at $\omega = \pm ja$ and $\omega = \pm jb$. The application of this filter is illustrated in Fig.1. The tracking signal shown in the red is decomposed into a slow signal shown in green, a medium speed signal shown in blue and a fast signal depicted in purple. The time-scale characteristics of the slow, medium and fast signals are respectively:

Hour: This time-scale is associated with the share of variations that are slow but have high levels of energy. Examples of phenomena causing deviations in this time-scale are errors in average cloud cover forecast which are typically provided by the National Weather Service in 1 to 3 hour-long intervals, or unpredicted failures in generation equipment. According to the slow rate of change, the sampling frequency that can capture this component can be in the order of a few minutes. The resources needed for the control purposes do not need to have a high ramp rate capacity, but they may need to have considerable amounts of power and energy capacities.

Minutes: This time-scale is the part of the problem which needs faster resources to respond, but not necessarily urging

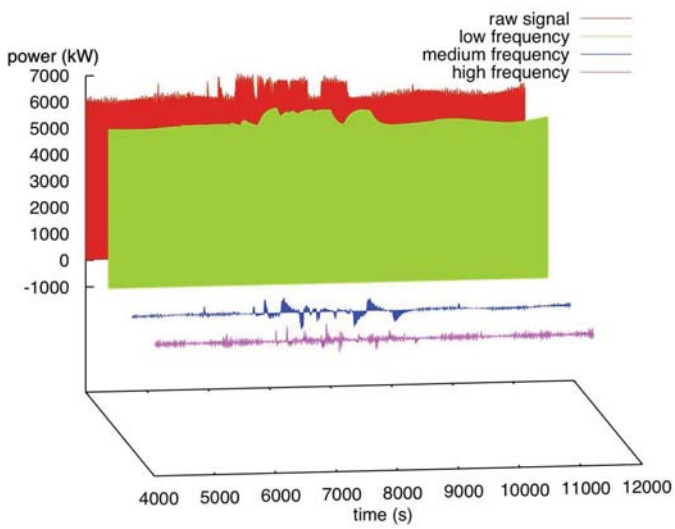

Fig. 1. Decomposition of an arbitrary signal. The low frequency component carries a higher level of energy, while the higher frequency content of the signal encompass small values of energy.

a significant energy capacity. Medium-speed deviations could be caused by demand-patterns or clouds intermittent occluding the sun. The sampling frequency in this time-scale should be in the order of about 10 seconds as highlighted in Fig.1.

Seconds: This category is addressing the portion of the deviations associated with the fastest fluctuations caused by start-up transient of devices or the edge of clouds passing in front of the sun. Thus, the sampling frequency is in the order of one second. The resources in this category need to have the highest ramp rates. However, the energy capacity can be relatively low.

Based on the above description, we consider a cascading control mechanism to follow a tracking signal. The decomposition component of the system subdivides the problem into three subproblems in order to reduce the computational costs. A schematic of this structure is shown in Fig. (2).

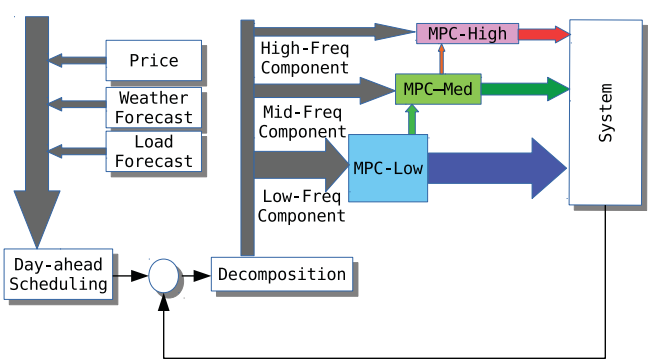

Fig. 2. Configuration of the studied control mechanism. The day-ahead scheduling optimized set points are adjusted throughout the day by cascading MPC structure.

In the cascading MPC framework, the low-frequency component of the tracking signal is addressed first. The time horizon for this component of the problem is 40 minutes discretized into 20 steps, each with a 120 seconds duration. Resources are allocated at each time step according to the solution of the optimization problem. The medium frequency tracking signal is obtained by first subtracting the low-frequency response from the master signal and then applying a band pass filter with appropriate range. The MPC algorithm dispatches medium frequency resources with the time horizons of 200 seconds discretized into 20 time intervals, each with 10 seconds duration. Finally, the high-frequency tracking signal is obtained by subtracting the low and medium responses from the master signal. Fast resources are similarly dispatched by the MPC process on the time horizons of 20 seconds discretized by 20×1-second time steps.

V. Numerical Results

We evaluate the ability of the proposed structure in a spinning reserves request problem. For this purpose, we use a real-time pricing (RTP) mechanism to affect the amount of load on the grid placed by the distribution feeder microgrid in question. The characteristics of the resources are brought in Table I, where we present a set of plausible specifications of resources that could be found on a distribution feeder, including conventional ones such as batteries, and unconventional ones such as load-following chillers, ventilation fans and TCLs. In addition, we assume that uncontrollable distributed generations, in the form of a large PV array, is present in the system.

We assume that the system is working based on a regular routine for which the day-ahead scheduling has been previously solved. However, as a result of a system level emergency, a rapid load-shed is requested from the microgrid. To achieve the desired result, the system operator enacts stepwise increase in the price of power from 8 AM to 10 AM. We assume for the purpose of emergency response, the utility is not able to provide advanced notice of energy prices.

The response of the microgrid to the assistance request is shown in Fig.3. The blue curve represents the scheduled power flow at the point of common coupling. The green curve represents actual power flow that would have occurred without an emergency request from the system. Finally, the red curve depicts the actual power flow as a result of the system load reduction request. In Fig.4, the total amount of power that the

TABLE I
Resource Characteristics

Resource	Power capacity	Energy capacity	Ramp rate
Energy Battery	[-250,250] KW	1000 KWH	1.67 %/sec
Chillers	[-150,150] KW	300 KWH	0.56 %/sec
Ventilation system	[-150,150] KW	300 KWH	20 %/sec
Ventilation system	[-50,50] KW	100 KWH	40 %/sec
TCLs	[-300,300] KW	25 KWH	100 %/sec

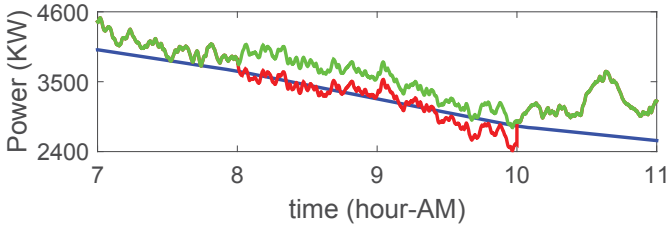

Fig. 3. The response of the system for a load reduction request from the utility; Blue: scheduled load at the coupling point, Green: actual demand in the absence of emergency request, and Red: reduced load at the common coupling point during the emergency.

microgrid was able to provide and the share of each resource is shown during the request period.

VI. Discussion

In this study we worked with 2 local resources in each mode of the MPC problem. In real, the number of resources can hypothetically increase to more than ten that consequently increases the computational cost. Due to the real-time nature of the problem, faster processors are essential, especially for higher frequencies.

We also showed that solutions to MPC problem can be obtained reliably using realistic cost functions. Additionally, separation of the reference signal into various frequency bands enabled us to save computational efforts, that can yield to extending the horizon of the dynamic programming problem to the order of an hour. This was done by increasing the sampling period, and achieving the essential performance without compromising system stability. As well as the computational cost, deploying non-conventional distributed resources made an opportunity to reduce the size of electrical storage.

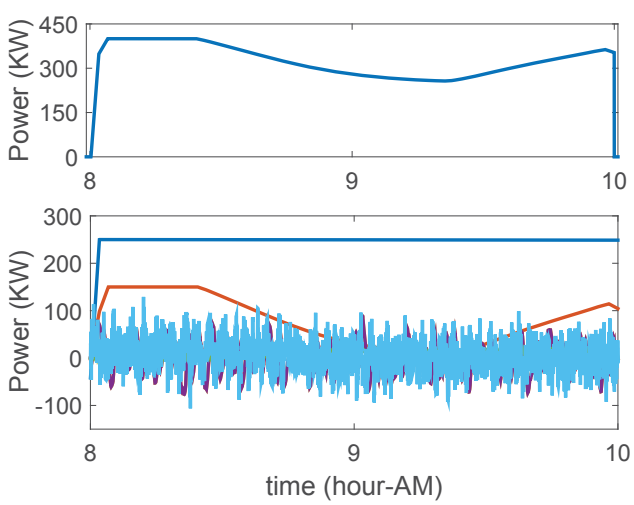

Fig. 4. Contribution of the microgrid to the demand reduction request. The upper plot depicts the total power that the microgrid was able to provide for supporting the utility (10% load reduction on average), and the bottom plot shows the share of each resource on the microgrid during the emergency situation. The bottom plot shows that the medium and high frequency components of the master signal are absorbed in the microgrid.

VII. Conclusion

In this paper, we used a new methodology implemented on a new architecture for the power system to integrate a wider range of distributed resources into the generation-mix. The cooperation between loads, generation and storage devices via an MPC mechanism could make it possible to reduce the size of electrical energy storage devices, and consequently the integration cost in a consistent way independent of the nature of the resources utilized. This is important as the share of intermittent renewable resources is increases.

The connected nature of future devices through ever-developing communication infrastructures also makes it possible to extend control levels over the loads. Thus, the proposed framework will enable utility companies to go beyond the current limits of deploying renewable resources on the grid. This increased level of control could also increase the resiliency of the whole grid against large failures. Application of this method showed that the optimization is treatable at the distribution level.

Acknowledgment

This work was supported by the Defense Threat Reduction Agency (DTRA) under grant number HDTRA1-13-1-0020. The authors wish to thank Mr. Mathew N. Robinson as well for his assistance in data acquisition used in this study.

References

[1] L. Che, M. Khodayar, and M. Shahidehpour, "Only connect: Microgrids for distribution system restoration," *Power and Energy Magazine, IEEE*, vol. 12, no. 1, pp. 70–81, 2014.

[2] P. Denholm and R. Margolis, "Very large-scale deployment of grid-connected solar photovoltaics in the united states: challenges and opportunities," *National Renewable Energy Laboratory*, 2006.

[3] A. Maitra, B. York, H. Kamath, T. Key, and V. Singhvi, "Microgrids: A primer," 2013.

[4] J. Mattingley, Y. Wang, and S. Boyd, "Receding horizon control," *Control Systems, IEEE*, vol. 31, no. 3, pp. 52–65, 2011.

[5] M. Arnold and G. Andersson, "Model predictive control of energy storage including uncertain forecasts," in *Power Systems Computation Conference (PSCC), Stockholm, Sweden*, 2011.

[6] J. L. Mathieu, S. Koch, and D. S. Callaway, "State estimation and control of electric loads to manage real-time energy imbalance," *Power Systems, IEEE Transactions on*, vol. 28, no. 1, pp. 430–440, 2013.

[7] Toshiba, "Toshiba today," 2011, corporate profile, micro-EMS (Energy Management System) for monitoring and controlling grids.

[8] R. Firestone, "Distributed energy resources customer adoption model technology data," *Berkeley Lab, Berkeley, CA, USA Case Study*, 2004.

[9] M. Grant and S. Boyd, "CVX: Matlab software for disciplined convex programming, version 2.1," Mar. 2014.

[10] ——, "Graph implementations for nonsmooth convex programs," in *Recent Advances in Learning and Control*, ser. Lecture Notes in Control and Information Sciences, V. Blondel, S. Boyd, and H. Kimura, Eds. Springer-Verlag Limited, 2008, pp. 95–110.

[11] W. H. Press, S. A. Teukolsky, W. T. Vetterling, and B. P. Flannery, "Numerical recipes in fortran," 1992.